

AUTOST: TRAINING-FREE NEURAL ARCHITECTURE SEARCH FOR SPIKING TRANSFORMERS

Ziqing Wang, Qidong Zhao, Jinku Cui, Xu Liu, Dongkuan Xu

North Carolina State University

ABSTRACT

Spiking Transformers have gained considerable attention because they achieve both the energy efficiency of Spiking Neural Networks (SNNs) and the high capacity of Transformers. However, the existing Spiking Transformer architectures, derived from Artificial Neural Networks (ANNs), exhibit a notable architectural gap, resulting in suboptimal performance compared to their ANN counterparts. Manually discovering optimal architectures is time-consuming. To address these limitations, we introduce `AutoST`, a training-free NAS method for Spiking Transformers, to rapidly identify high-performance Spiking Transformer architectures. Unlike existing training-free NAS methods, which struggle with the non-differentiability and high sparsity inherent in SNNs, we propose to utilize Floating-Point Operations (FLOPs) as a performance metric, which is independent of model computations and training dynamics, leading to a stronger correlation with performance. Our extensive experiments show that `AutoST` models outperform state-of-the-art manually or automatically designed SNN architectures on static and neuromorphic datasets. Full code, model, and data are released for reproduction.¹

Index Terms— Spiking Neural Network, Transformer, Neural Architecture Search

1. INTRODUCTION

Spiking neural networks (SNNs) have gained extensive attention owing to their remarkable energy efficiency [1]. Concurrently, the Transformer has exhibited impressive performance in a wide array of computer vision tasks [2, 3]. This has led to a growing interest in integrating SNNs with Transformers to develop Spiking Transformers, which makes it possible to achieve high energy efficiency and superior performance [4, 5].

Despite these successes, existing Spiking Transformer architectures predominantly rely on ANN-based architectures. This dependence tends to overlook the unique properties of SNNs, resulting in less optimal performance compared to their ANN counterparts [6, 7]. As illustrated in Fig. 1, there is a substantial variation in accuracy and energy consumption across different SNN architectures. This variation highlights the need for a more in-depth investigation of the design choices of Spiking Transformer architectures.

Finding optimal SNN architectures has traditionally been pursued via two common approaches. The first involves manually designing architectures, which is a labor-intensive endeavor [6] and does not guarantee optimal results [8]. The second approach involves utilizing Neural Architecture Search (NAS) methods to automatically discover the ideal architecture. However, most existing NAS methods require multiple training stages or a single supernet training that encompasses all architecture candidates [9], leading to longer convergence

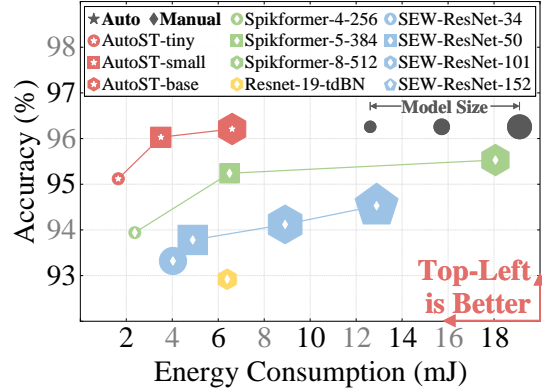


Fig. 1: Comparison between `AutoST` and state-of-the-art SNN models on the CIFAR-10 dataset. The marker sizes represent the model sizes. Star-shaped and diamond-shaped hollows within the markers denote manually and automatically designed models, respectively.

times compared to standard training. Considering that the SNNs generally exhibit slower training speeds compared to their ANN counterparts [6], the application of these NAS methods to SNNs is challenging.

To address these limitations, we propose, for the first time, to leverage training-free NAS to rapidly identify high-performance Spiking Transformer architectures. Recent training-free NAS approaches [8], which search for the optimal architecture from initialized networks without any training, substantially reduce search times. Nevertheless, it is not straightforward to directly apply these existing training-free NAS methods to Spiking Transformers. Most current methods, developed for ANNs, rely on gradients during a backward pass; however, the spike is non-differentiable during backpropagation in SNNs, leading to inaccurate gradients. Moreover, methods employing activation patterns introduce significant errors due to the inherent high sparsity of SNNs [6].

In this work, we propose `AutoST`, a training-free NAS to search for superior Spiking Transformer architectures. Our approach utilizes Floating-Point Operations (FLOPs) as a performance metric, which is independent of model computations and training dynamics, thus effectively tackling the challenges posed by non-differentiability and high sparsity inherent to SNNs, leading to a stronger correlation with performance. To the best of our knowledge, `AutoST` is the first implementation of training-free NAS to explore Spiking Transformer architectures. Extensive experiments show that our searched `AutoST` models outperform state-of-the-art SNNs on both static and neuromorphic datasets. In particular, the accuracy of our `AutoST` model outperforms that of the SNN models searched by other NAS methods by 3.06%, 4.34%, and 9.10% on the CIFAR-10, CIFAR-100, and CIFAR10-DVS, respectively.

¹<https://github.com/AlexandreWANG915/AutoST>

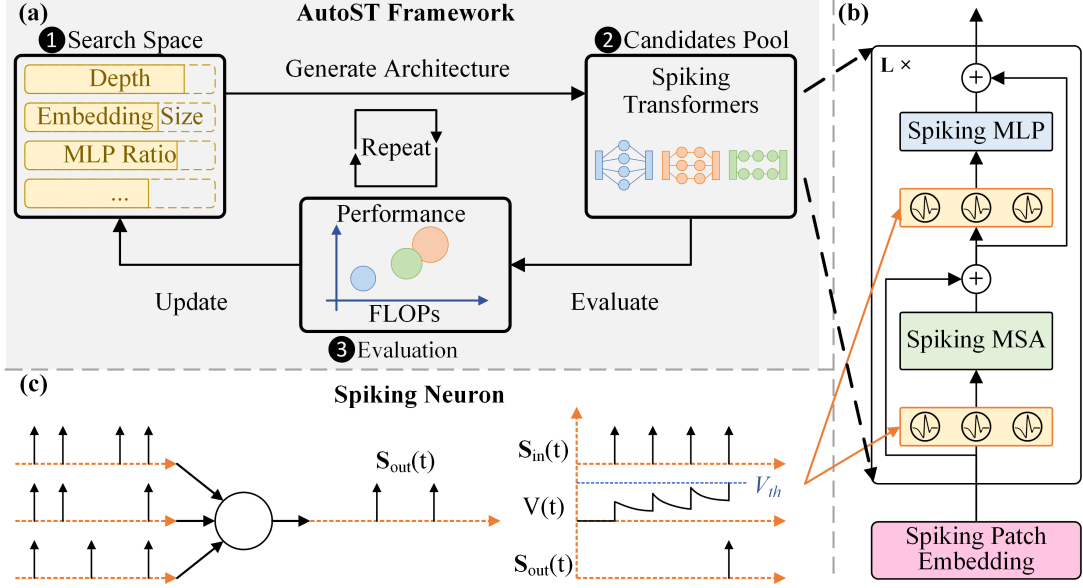


Fig. 2: Overview of AutoST . Subfigure (a) shows the AutoST pipeline: ① Initial generation of architecture candidates within a predefined search space; ② Selection of Spiking Transformer architectures from the candidate pool; ③ Evaluation of selected architectures based on proposed training-free metrics. Subfigure (b) presents the overall architecture of Spiking Transformers. Subfigure (c) illustrates the operation of a spiking neuron, which transmits spikes to the subsequent layer when the membrane potential $V(t)$ surpasses the threshold V_{th} .

2. PRELIMINARY

2.1. Spiking Neuron Model

Unlike traditional ANNs, SNNs utilize binary spike trains to convey information. As shown in Fig. 2, we employ the widely adopted Leaky-Integrate-and-Fire (LIF) model to mimic the dynamics of spiking neurons. The LIF model is defined as follows:

$$H[t] = V[t-1] + \frac{1}{\tau} (X[t] - (V[t-1] - V_{\text{reset}})), \quad (1)$$

$$S[t] = \Theta(H[t] - V_{th}), \quad (2)$$

$$V[t] = H[t](1 - S[t]) + V_{\text{reset}} S[t], \quad (3)$$

where τ denotes the membrane time constant, $X[t]$ represents the input current at the timestep t . When the membrane potential $V[t]$ exceeds the firing threshold V_{th} at the timestep t , a spike $S[t]$ will be generated by the spiking neuron to the next layer. The Heaviside step function $\Theta(v)$ equals 1 for $v \geq 0$ and 0 otherwise. $V[t]$ represents the membrane potential post the triggering event, which equals $H[t]$ if no spike is produced and is otherwise reset to the potential V_{reset} .

3. TRAINING-FREE NAS FOR SPIKING TRANSFORMERS

3.1. Performance Prediction via FLOPs

In this section, we first explore the application of recent training-free metrics for NAS in the context of Spiking Transformers. Many existing metrics require forward and backward passes through the architecture to compute a score, such as SynFlow [10], Snip [11] and NTK [12].

However, SNNs undergo a Heaviside step function during forward propagation, leading to non-differentiability during backward propagation. This intrinsic characteristic of SNNs can result in inaccurate gradient calculations and potentially unreliable metric scores. Furthermore, while the LinearRegions method [13] circumvents the

need for a backward pass, it faces challenges due to large variations in the sparsity of activation patterns in SNNs [6]. These variations in sparsity impact the suitability of the LinearRegions method for Spiking Transformers. To overcome these constraints, we propose the use of FLOPs as a metric to predict the final performance of the model. This approach is solely related to the self-characterization of the model and eliminates the need for forward/backward propagation, effectively circumventing both the non-differentiability and sparsity variation issues.

The computation of FLOPs in a Transformer model is predominantly attributed to two components: the Self Attention (SA) block and the Multi-layer Perceptron (MLP) block. We present the computation for each component as follows:

$$\text{FLOPs}_{\text{MSA}} = L \times n \times d_{\text{model}} \times (2d_{\text{model}} + n) \quad (4)$$

$$\text{FLOPs}_{\text{MLP}} = L \times n \times (d_{\text{model}} \times d_{\text{mlp}} + d_{\text{mlp}} \times d_{\text{model}}) \quad (5)$$

For the SA block, FLOPs_{SA} denotes the total number of floating-point operations required, where L represents the number of layers, n the sequence length, and d_{model} is the embedding dimension of the model. For the MLP block, d_{mlp} represents the hidden dimension.

The computation of the FLOPs of Spiking Transformers is similar to the process for ANN Transformers, with additional consideration for the time dimension. To account for this, we multiply the FLOPs of the ANN-equivalent architecture by the number of timesteps: $\text{FLOPs}_{\text{SNN}} = T \times \text{FLOPs}_{\text{ANN}}$.

To demonstrate the effectiveness of our proposed metric, AutoST , we randomly sample 100 architectures from the small search space outlined in Tab. 2. We initially train these architectures for 100 epochs, compute the training-free metric scores, and then analyze their correlation with the final model performance. As shown in Tab. 1 and Fig. 3, our AutoST has high absolute values for both Kendall and Spearman coefficients. This suggests that the FLOPs metric has a strong correlation with model performance. This correlation is largely due to two factors. First, the FLOPs metric is

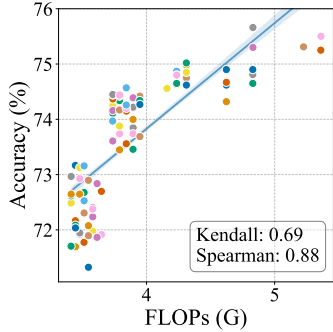


Fig. 3: Performance Metric Evaluation: Evidence of a significant positive correlation between FLOPs and accuracy.

Table 1: Comparison of Correlation Coefficients: Analysis of the proposed metric against different training-free metrics. Note that absolute values of Kendall and Spearman coefficients approaching one indicate a stronger correlation between two variables. The search time represents the duration required to search 200 samples on the CIFAR-100 dataset with a single GPU. Our metric exhibits a pronounced correlation with the final accuracy.

Datasets	CIFAR-10		CIFAR-100	
	Kendall	Spearman	Kendall	Spearman
NTK [12]	-0.43	-0.49	-0.40	-0.55
Snyflow [10]	0.57	0.77	0.56	0.76
LinearRegions [13]	0.58	0.85	0.59	0.79
SAHD [6]	0.56	0.81	0.52	0.74
AutoST (ours)	0.70	0.91	0.69	0.88

independent of gradients, which allows it to circumvent the inherent non-differentiability of SNNs. Second, previous works assessed their metrics over a large parameter range, whereas, real-world applications often demand the identification of the optimal model within specific constraints (e.g., 4-5 M). In such circumstances, traditional metrics struggle to distinguish model differences in such a narrow parameter range. In contrast, AutoST using FLOPs can effectively distinguish different models due to its calculation based on layer numbers and embedding dimensions.

3.2. Overall Architecture of AutoST

The overall architecture of AutoST is based on [4], a purely transformer-based SNN. The overview of AutoST is depicted in Fig. 2. Considering an input 2D image sequence $I \in \mathbb{R}^{T \times C \times H \times W}$, a Spiking Patch Embedding (SPE) block is utilized for downsampling and partitioning the input into spiking patches $X \in \mathbb{R}^{T \times N \times D}$. These patches are subsequently passed through L Spiking Transformer Blocks, each comprising a Spiking Self Attention (SSA) block and a Spiking MLP (SMLP) block. The final stage consists of a Global Average Pooling (GAP) and a Fully Connected Layer (FC) serving as the classification head, outputting the prediction Y . The sequence of operations is mathematically defined as follows:

$$X = \text{SPE}(I), \quad I \in \mathbb{R}^{T \times C \times H \times W}, \quad X \in \mathbb{R}^{T \times N \times D} \quad (6)$$

$$X'_l = \text{SSA}(X_{l-1}) + X_{l-1}, \quad X'_l \in \mathbb{R}^{T \times N \times D}, \quad l = 1 \dots L \quad (7)$$

$$X_l = \text{SMLP}(X'_l) + X'_l, \quad X_l \in \mathbb{R}^{T \times N \times D}, \quad l = 1 \dots L \quad (8)$$

$$Y = \text{FC}(\text{GAP}(X_L)) \quad (9)$$

3.3. Search Space and Search Algorithm of AutoST

We design an extensive search space for AutoST, comprising four key variables in the Transformer: embedding size, number of heads, MLP ratio, and network depth, as detailed in Tab. 2. Based on these five variables, we design three distinct search spaces (Tiny, Small, and Base) for AutoST. Given the constraints on the model parameters, we divide the large-scale search space into three parts, as described in Tab. 2. This partitioning enables the search algorithm to focus on discovering models within a specific parameter range. And we conduct an evolutionary search to obtain the optimal AutoST under specified resource constraints.

Table 2: The search space of AutoST. Tuples in parentheses represent the lowest, highest value, and steps.

	AutoST-tiny	AutoST-small	AutoST-base
Embed Size	(192, 384, 64)	(256, 512, 64)	(384, 768, 64)
MLP Ratio	(3, 5, 1)	(3, 5, 1)	(3, 6, 1)
Head Num	(4, 8, 4)	(4, 8, 4)	(4, 8, 4)
Depth	(1, 8, 1)	(2, 12, 1)	(4, 15, 1)
# Params	4-5M	11-15M	25-35M

4. EXPERIMENTS

4.1. Performance on CIFAR Datasets

Tiny Models. AutoST surpasses both Spikformer [4] and AutoSNN [14]. Specifically, the proposed AutoST surpasses AutoSNN, which is obtained through NAS, by 2.6%, 10.1%, and 13.01% on three datasets with fewer parameters and timesteps. This indicates that our model leverages the efficient search space of the AutoST, allowing for enhanced performance with reduced model complexity. **Small Models.** The larger search space provides additional flexibility, potentially enhancing performance. Our AutoST outperforms Spikformer [4] in the same parameter range and yields higher accuracy compared to CNN-based models. Remarkably, AutoST not only outperforms the current state-of-the-art SNN model, DSR [17], in terms of accuracy but also demonstrates significantly fewer time steps, leading to lower SNN latency. This performance suggests that our AutoST method of utilizing an expanded search space can lead to significant performance gains in SNN architectures. **Base Models.** AutoST maintains its superior performance, outperforming all other models with substantially fewer parameters in a larger search space. This further highlights the effectiveness and efficiency of our proposed method, potentially opening new avenues for SNN.

4.2. Performance on ImageNet Dataset

In Tab. 4, we showcase the performance of several models on the ImageNet dataset. The SEW ResNet [20] model has two variations: SEW-ResNet-50 with 25.56M parameters (67.04% accuracy) and SEW-ResNet-101 with 44.55M parameters (67.78% accuracy). The Spikformer [4] model offers configurations like Spikformer-6-256 (5.99M parameters, 62.99% accuracy) and scaled-up versions Spikformer-8-384 and Spikformer-10-512, achieving accuracies of 70.24% and 73.68% respectively. Our proposed AST model, AutoST, demonstrates a competitive performance-to-parameter ratio. Notably, AutoST-small, with only 14.68M parameters, outperforms Spikformer-8-384 with an accuracy of 71.02%. The AutoST-base configuration achieves the highest accuracy of 74.54% among all models in the table with its 34.44M parameters. In essence, AutoST delivers outstanding performance on large-scale datasets.

Table 3: Performance comparison between the proposed `AutoST` model and the state-of-the-art models on the CIFAR-10 and CIFAR-100 datasets. * represent the result of our implementation. Acc. denotes the top-1 accuracy.

Methods	# Param (M)	Timesteps	CIFAR-10 Acc. (%)	CIFAR-100 Acc. (%)	Model Type	Design Type
Spikformer-4-256 [4] [ICLR23]	4.15	4	93.94	75.96	Transformer	Manual
AutoSNN [14] [ICML22]	5.44	8	92.54	69.16	CNN	Auto
SNASNet-Bw [15] [ECCV22]	-	5	93.64	73.04	CNN	Auto
<code>AutoST</code> -tiny (ours)	4.20	4	95.14	76.29	Transformer	Auto
TET [16] [ICLR22]	12.60	6	94.50	74.72	CNN	Manual
DSR [17] [CVPR22]	11.20	20	95.40	78.20	CNN	Manual
Spikformer-5-384* [4] [ICLR23]	11.32	4	95.24	78.12	Transformer	Manual
SpikeDHS [14] [CVPR23]	12.00	6	94.34	75.70	CNN	Auto
<code>AutoST</code> -small (ours)	11.52	4	96.03	79.44	Transformer	Auto
Diet-SNN [18] [TNNLS21]	39.90	5	93.44	69.67	CNN	Manual
RMP [19] [CVPR20]	39.90	2048	93.63	70.93	CNN	Manual
Spikformer-8-512* [4] [ICLR23]	29.68	4	95.53	78.48	Transformer	Manual
<code>AutoST</code> -base (ours)	29.64	4	96.21	79.69	Transformer	Auto

Table 4: Performance comparison on the ImageNet dataset.

Methods	# Param (M)	Ts	Architecture	Acc (%)
SEW ResNet [20]	25.56	6	SEW-ResNet-50	67.04
	44.55		SEW-ResNet-101	67.78
Spikfomer [4]	5.99	4	Spikformer-6-256	62.99
	16.81		Spikformer-8-384	70.24
	29.68		Spikformer-10-512	73.68
<code>AutoST</code> (ours)	5.99	4	<code>AutoST</code> -tiny	63.80
	14.68		<code>AutoST</code> -small	71.02
	34.44		<code>AutoST</code> -base	74.54

Table 5: Performance comparison on the CIFAR10-DVS dataset.

Methods	Timesteps	Acc (%)	Model Type	Design Type
tdBN [20]	10	67.8	CNN	Manual
LIAF-Net [21]	10	70.4	CNN	Manual
PLIF [22]	20	74.8	CNN	Manual
Dspkie [23]	10	75.4	CNN	Manual
DSR [17]	10	77.3	CNN	Manual
SEW-ResNet [20]	16	74.4	CNN	Manual
Spikformer [4]	16	80.9	Transformer	Manual
AutoSNN [14]	8	72.5	CNN	Auto
<code>AutoST</code> (ours)	16	81.6	Transformer	Auto

4.3. Performance on Neuromorphic Datasets

We further demonstrate the superiority of the `AutoST` method by evaluating its performance on neuromorphic datasets. We compare our model with state-of-the-art SNN models on the CIFAR10-DVS dataset. Due to the overfitting issue on neuromorphic datasets, we restrict our comparison to the tiny model. Tab. 5 reveals that the `AutoST` model achieves the highest top-1 accuracy, outperforming the existing state-of-the-art SNN models. Notably, `AutoST` outperforms SEW-ResNet [20] by 7.2% while maintaining far fewer parameters. These results further validate the effectiveness of our proposed method and its strong generalization capabilities when applied to neuromorphic datasets.

4.4. Analysis of Model Topology and Timestep Optimization

Timestep Optimization. As depicted in Fig. 4a, there is a discernible positive correlation between the number of timesteps and the performance of the model. While an increase in timesteps tends to enhance

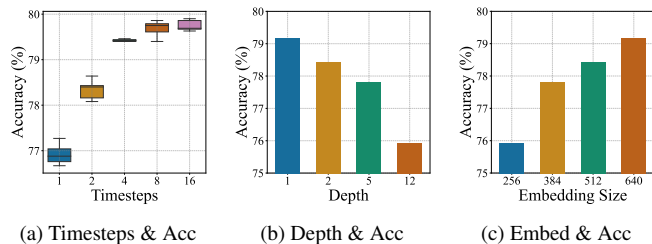


Fig. 4: Subfigure (a) reveals that timesteps and accuracy have a positive correlation. Subfigure (a-c) highlights the advantages of the search `AutoST` architectures: higher accuracy, lower training time, increased FLOPs, and decreased power consumption.

accuracy, it concomitantly leads to greater latency and energy consumption. Through our analysis, a timestep value of 4 emerges as a pivotal point that amplifies accuracy without compromising efficiency, thus serving as our preferred choice for subsequent experiments.

Model Topology Insights. Our exploration into the search rule of `AutoST` has unveiled an inclination towards network structures that are shallower yet broader, marking a distinct shift from the conventional preference of SNNs for configurations that are deeper and narrower [24]. To validate this observation, we manually crafted and assessed four distinct architectures, varying in embedding sizes and depths but within a similar parameter range. Figures 4b-4c corroborate our hypothesis, indicating that architectures with increased width consistently outperform their counterparts in terms of accuracy. This phenomenon is likely attributable to the intrinsic characteristics of SNNs. Specifically, architectures that are broader but not as deep can mitigate the accumulation of quantization errors across layers [25]. This observed predilection for broader Transformers aligns well with recent scholarly insights [26].

5. CONCLUSION

In this paper, we introduce `AutoST`, a training-free NAS method for Spiking Transformers. Our unique approach of utilizing Floating-Point Operations (FLOPs) as a performance metric bypasses the non-differentiability and high sparsity issues present in SNNs. Empirical results confirm that `AutoST` models consistently outperform both manual and other automatic SNN architectures across diverse datasets. In essence, `AutoST` paves the way for optimizing Spiking Transformers, promising enhanced performance and efficiency.

6. REFERENCES

- [1] Wolfgang Maass, “Networks of spiking neurons: The third generation of neural network models,” *Neural networks*, vol. 10, no. 9, pp. 1659–1671, 1997.
- [2] Alexey Dosovitskiy, Lucas Beyer, Alexander Kolesnikov, Dirk Weissenborn, Xiaohua Zhai, Thomas Unterthiner, Mostafa Dehghani, Matthias Minderer, Georg Heigold, and Sylvain Gelly, “An image is worth 16x16 words: Transformers for image recognition at scale,” *arXiv preprint arXiv:2010.11929*, 2020.
- [3] Ze Liu, Yutong Lin, Yue Cao, Han Hu, Yixuan Wei, Zheng Zhang, Stephen Lin, and Baining Guo, “Swin transformer: Hierarchical vision transformer using shifted windows,” in *Proceedings of the IEEE/CVF International Conference on Computer Vision*, 2021, pp. 10012–10022.
- [4] Zhaokun Zhou, Yuesheng Zhu, Chao He, Yaowei Wang, Shuicheng Yan, Yonghong Tian, and Li Yuan, “Spikformer: When Spiking Neural Network Meets Transformer,” *arXiv preprint arXiv:2209.15425*, 2022.
- [5] Ziqing Wang, Yuetong Fang, Jiahang Cao, Zhongrui Wang, and Renjing Xu, “Efficient Spiking Transformer Enabled By Partial Information,” Oct. 2022, arXiv:2210.01208 [cs].
- [6] Youngeun Kim, Yuhang Li, Hyungseob Park, Yeshwanth Venkatesha, and Priyadarshini Panda, “Neural architecture search for spiking neural networks,” in *Computer Vision—ECCV 2022: 17th European Conference, Tel Aviv, Israel, October 23–27, 2022, Proceedings, Part XXIV*. 2022, pp. 36–56, Springer.
- [7] Byunggook Na, Jisoo Mok, Seongsik Park, Dongjin Lee, Hyeokjun Choe, and Sungroh Yoon, “AutoSNN: Towards energy-efficient spiking neural networks,” in *International Conference on Machine Learning*. 2022, pp. 16253–16269, PMLR.
- [8] Qingqin Zhou, Kekai Sheng, Xiawu Zheng, Ke Li, Xing Sun, Yonghong Tian, Jie Chen, and Rongrong Ji, “Training-free transformer architecture search,” in *Proceedings of the IEEE/CVF Conference on Computer Vision and Pattern Recognition*, 2022, pp. 10894–10903.
- [9] Han Cai, Ligeng Zhu, and Song Han, “Proxylessnas: Direct neural architecture search on target task and hardware,” *arXiv preprint arXiv:1812.00332*, 2018.
- [10] Hidenori Tanaka, Daniel Kunin, Daniel L. Yamins, and Surya Ganguli, “Pruning neural networks without any data by iteratively conserving synaptic flow,” *Advances in neural information processing systems*, vol. 33, pp. 6377–6389, 2020.
- [11] Namhoon Lee, Thalaisyasingam Ajanthan, and Philip HS Torr, “Snip: Single-shot network pruning based on connection sensitivity,” *arXiv preprint arXiv:1810.02340*, 2018.
- [12] Arthur Jacot, Franck Gabriel, and Clément Hongler, “Neural tangent kernel: Convergence and generalization in neural networks,” *Advances in neural information processing systems*, vol. 31, 2018.
- [13] Joe Mellor, Jack Turner, Amos Storkey, and Elliot J. Crowley, “Neural architecture search without training,” in *International Conference on Machine Learning*. 2021, pp. 7588–7598, PMLR.
- [14] Shu Miao, Guang Chen, Xiangyu Ning, Yang Zi, Kejia Ren, Zhenshan Bing, and Alois Knoll, “Neuromorphic vision datasets for pedestrian detection, action recognition, and fall detection,” *Frontiers in neurorobotics*, vol. 13, pp. 38, 2019.
- [15] Tong Bu, Wei Fang, Jianhao Ding, PengLin Dai, Zhaofei Yu, and Tiejun Huang, “Optimal ANN-SNN Conversion for High-accuracy and Ultra-low-latency Spiking Neural Networks,” in *International Conference on Learning Representations*, 2021.
- [16] Shikuang Deng, Yuhang Li, Shanghang Zhang, and Shi Gu, “Temporal Efficient Training of Spiking Neural Network via Gradient Re-weighting,” *arXiv preprint arXiv:2202.11946*, 2022.
- [17] Qingyan Meng, Mingqing Xiao, Shen Yan, Yisen Wang, Zhouchen Lin, and Zhi-Quan Luo, “Training High-Performance Low-Latency Spiking Neural Networks by Differentiation on Spike Representation,” in *Proceedings of the IEEE/CVF Conference on Computer Vision and Pattern Recognition*, 2022, pp. 12444–12453.
- [18] Nitin Rathi and Kaushik Roy, “DIET-SNN: Direct Input Encoding With Leakage and Threshold Optimization in Deep Spiking Neural Networks,” Dec. 2020.
- [19] Bing Han, Gopalakrishnan Srinivasan, and Kaushik Roy, “Rmp-snn: Residual membrane potential neuron for enabling deeper high-accuracy and low-latency spiking neural network,” in *Proceedings of the IEEE/CVF Conference on Computer Vision and Pattern Recognition*, 2020, pp. 13558–13567.
- [20] Hanle Zheng, Yujie Wu, Lei Deng, Yifan Hu, and Guoqi Li, “Going deeper with directly-trained larger spiking neural networks,” in *Proceedings of the AAAI Conference on Artificial Intelligence*, 2021, vol. 35, pp. 11062–11070.
- [21] Zhenzhi Wu, Hehui Zhang, Yihan Lin, Guoqi Li, Meng Wang, and Ye Tang, “Liaf-net: Leaky integrate and analog fire network for lightweight and efficient spatiotemporal information processing,” *IEEE Transactions on Neural Networks and Learning Systems*, vol. 33, no. 11, pp. 6249–6262, 2021.
- [22] Wei Fang, Zhaofei Yu, Yanqi Chen, Timothée Masquelier, Tiejun Huang, and Yonghong Tian, “Incorporating learnable membrane time constant to enhance learning of spiking neural networks,” in *Proceedings of the IEEE/CVF International Conference on Computer Vision*, 2021, pp. 2661–2671.
- [23] Yuhang Li, Yufei Guo, Shanghang Zhang, Shikuang Deng, Yongqing Hai, and Shi Gu, “Differentiable spike: Rethinking gradient-descent for training spiking neural networks,” *Advances in Neural Information Processing Systems*, vol. 34, pp. 23426–23439, 2021.
- [24] Hanle Zheng, Yujie Wu, Lei Deng, Yifan Hu, and Guoqi Li, “Going Deeper With Directly-Trained Larger Spiking Neural Networks,” Dec. 2020.
- [25] Tong Bu, Wei Fang, Jianhao Ding, PengLin Dai, Zhaofei Yu, and Tiejun Huang, “Optimal ANN-SNN Conversion for High-accuracy and Ultra-low-latency Spiking Neural Networks,” in *International Conference on Learning Representations*, 2021.
- [26] Xiaohua Zhai, Alexander Kolesnikov, Neil Houlsby, and Lucas Beyer, “Scaling vision transformers,” in *Proceedings of the IEEE/CVF Conference on Computer Vision and Pattern Recognition*, 2022, pp. 12104–12113.